Conf-9404100--C

LA-UR- 94-1888

Title: STOCHASTIC SOURCE COMPARISONS BETWEEN NUCLEAR AND CHEMICAL EXPLOSIONS DETONATED AT RAINIER MESA, NEVADA TEST SITE

Author(s): Brian W. Stump
Robert E. Reinke

Submitted to: Proceedings of the symposium on the Non-Proliferation Experiment results and implications, M. D. Denny, Editor Lawrence Livermore National Laboratory, Livermore, CA Conf-940400

Los Alamos
NATIONAL LABORATORY

STOCHASTIC SOURCE COMPARISONS BETWEEN NUCLEAR AND CHEMICAL EXPLOSIONS DETONATED AT RAINIER MESA, NEVADA TEST SITE

Brian W. Stump
D. Craig Pearson
Geophysics Group, EES-3, MS-C335
Los Alamos National Laboratory
Los Alamos, NM 87545

Robert E. Reinke
Field Command Defense Nuclear Agency
1680 Texas St. SE
Kirtland AFB, NM 87117

I. INTRODUCTION/MOTIVATION

Seismic source functions are used to quantify the generation of body and surface waves from a wide variety of physical phenomena. Careful quantification of the relative excitation of the different seismic phases can be used to identify the source type. The geometry of the source has a strong influence on the types of waves a particular source generates. The different source types include earthquakes which are considered deviatoric in nature and explosions which are represented in their simplest form as isotropic or spherically symmetric. The deviatoric characteristic of earthquakes leads to efficient generation of shear waves while the symmetry of the contained spherical explosion results in primarily P wave excitation. Cylindrical explosive sources, typically found in the mining industry, result in reduced symmetry and somewhat enhanced shear wave generation although not as efficiently as that found from earthquakes. Identification of a source as a spherical explosion, cylindrical explosion or earthquake is partially dependent on these geometrical properties of the different source types.

Theory predicts that these different source types will have characteristically different time functions as well. A number of empirical discriminants for earthquakes and explosions are dependent upon the relative excitation of different frequency components of regional seismic phases. By combining these time or frequency domain effects with the geometrical excitation the most robust discriminants can be developed.

The focus of this study is the understanding of the time function effects for chemical and nuclear explosion sources detonated in a spherical geometry. Information developed here in combination with similar studies for earthquakes and mining explosions will be used to improve current discriminants, address the transportability of the discriminants to new regions and suggest new discriminants utilizing current data sources. The quantification of the seismic source time function for nuclear and chemical explosions provides the basis for identifying source differences that may develop as a function of yield as well as explosive type (chemical or nuclear). The yield effects are useful in yield determination as well as assessing detection and identification capabilities if seismic monitoring of such sources is important. Source effects attributable to yield can be used to establish new or verify existing scaling relations.

The characterization of the seismic source function can be completed in the time or frequency domain. Time domain characterization not only quantifies the total source strength but also how it is distributed in time. Frequency domain representations provide the ability to identify static offsets of the source, characteristic frequency associated with the physical size of the source and the smoothness of the energy deposition or high frequency decay. In the case of frequency domain representations the phase of the signal can either be included or discarded in the analysis. Ignoring the phase information in the source precludes the ability to track the distribution of source information as a function of time and as such is more restrictive.

The data that is utilized in this chemical/nuclear explosion source function study has been recovered from the free surface in the near-source region. As in all seismological studies, the observed data is linearly dependent upon both the propagation and source contributions. This study focuses on near-source data to maximize the bandwidth over which the source comparison can be made and to make any propagation path corrections as simple as possible. It is well known that local receiver effects on observed waveforms can be quite strong. In order to mitigate these effects in a comparative way all the explosions sources were observed with a consistent set of receivers.

II. PROBLEM DEFINITION

An experimental program was begun five years ago to define the equivalent elastic source function for nuclear explosions. The NPE provided the opportunity to extend this investigation to chemical sources as well. As part of these integrated investigations, free-field (Olsen and Perrat, These Proceedings) and free surface (Reinke et al., These Proceedings) observations were made on the nuclear explosions MISTY ECHO (ME, 10 DEC 88), MINERAL QUARRY (MQ, 25 July 90), HUNTERS TROPHY (HT, 18 Sept 92) and the chemical explosions NON-PROLIFERATION EXPERIMENT (NPE, 22 Sept 93) and NON-PROLIFERATION EXPERIMENT CALIBRATION (NPE CAL, 30 Oct 92) (Figure 1). The combination of free-field, free surface near-source network and free-surface tight array (8-80m) provides a unique opportunity for separation of propagation path effects from source processes. The range of different types of sources (chemical and nuclear) and different yields ($\sim 10^2$ to 10^6 lb. equivalent TNT) provides data for characterizing source dominated processes that may be important in monitoring and identifying explosions in other environments.

The characterization of the free surface data and quantification of propagation path effects is given in the paper by Reinke et al., these proceedings. The results of the free surface near-source network and free surface tight array analysis indicate that at relatively low frequencies (<10 Hz) that stochastic propagation effects are important
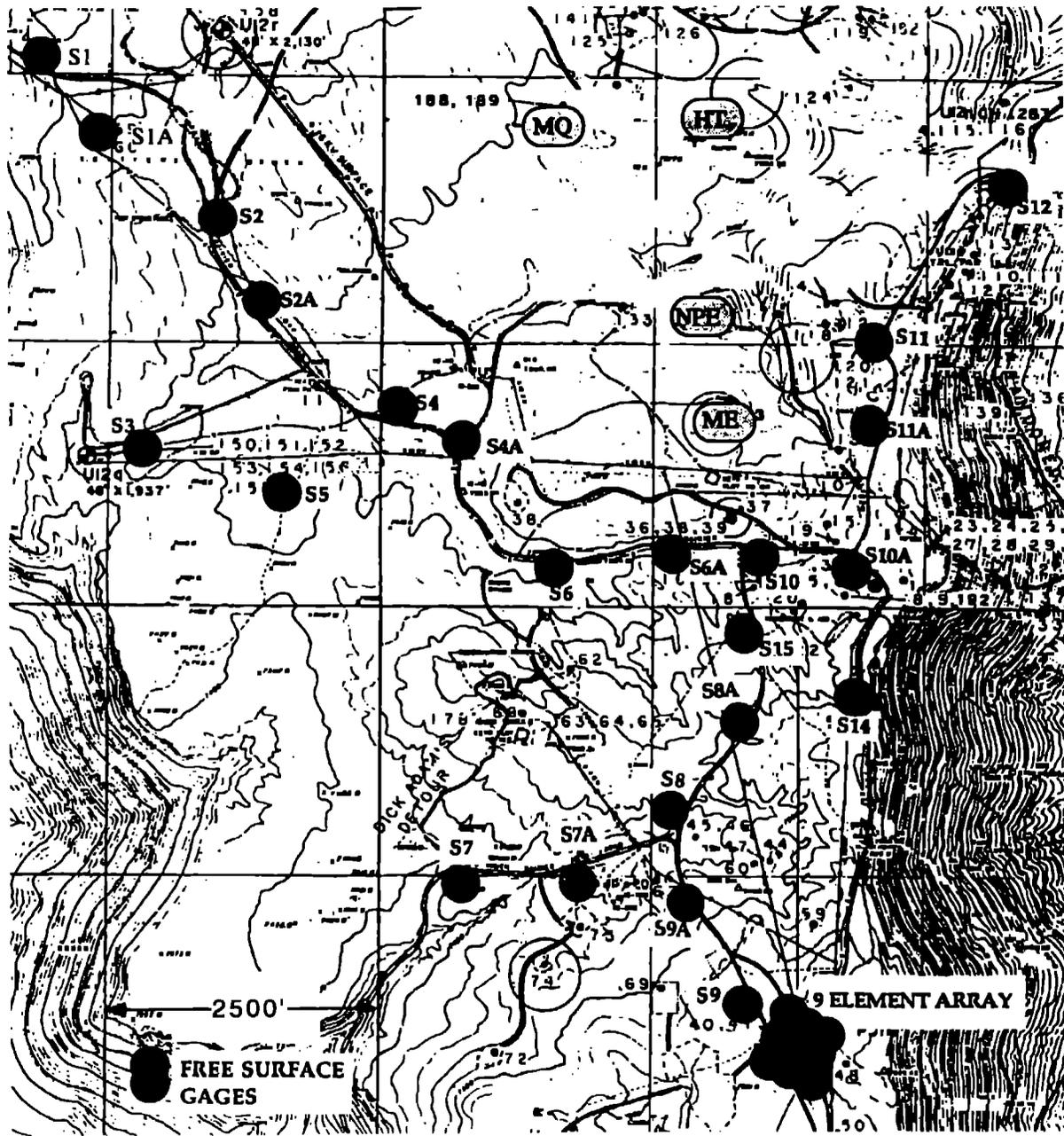
Figure 1: Rainier Mesa near-source free surface array for the experiments Misty Echo (ME), Mineral Quarry (MQ), Hunters Trophy (HT), Non-Proliferation Experiment (NPE) and NPE CAL (same location as NPE).

contributors to the observed waveforms (0.5-3.0 km range). The large scatter in the peak, near-source velocity data (Figure 2) is the simplest expression of this characteristic. Based upon this analysis and interpretation, a *stochastic* approach to source comparisons was designed and implemented.

This study makes no use of the signal phase but instead makes frequency domain comparisons of power spectral estimates. Implicit in this analysis is the importance of smoothing to reduce variances in the estimates. The variance reduction takes the form of averaging over neighboring frequency points for a single estimate and over multiple observations for the same source.

The focus is the identification of relative source differences as evidenced by the experimental data. The range of different source types and sizes allows constraint of the following aspects of the explosion source model:

   A. CHEMICAL/NUCLEAR SOURCE SIMILARITIES AND DIFFERENCES (*NPE* TO *HT* COMPARISON, Section III of this paper).

   B. UTILITY OF SMALL SCALE CALIBRATION EXPLOSIONS FOR SOURCE QUANTIFICATION (*NPE CAL TO NPE* COMPARISON, Section IV).

   C. EXPLOSION SOURCE SCALING OF SMALL YIELD NUCLEAR EXPLOSIONS (*HT* TO *MQ* COMPARISON, Section V).

The observations from this study were made in and on Rainier Mesa above the N-tunnel complex (Figure 1). The surface instrumentation consisted of force-balance accelerometers (f_c > 100 Hz) and Sprengnether S-6000, 2 Hz velocity sensors recorded by Refraction Technology 16 bit and Terra Technology 12 bit digital acquisition systems. Timing and location were provided by a combination of WWVB, GOES and GPS receivers. It is important to emphasize that for the MQ, HT, NPE CAL and NPE sources an identical set of receiver sites were used thus eliminating apparent source differences that are actually attributable to local receiver structure. Since the sources themselves are at different spatial locations (except NPE CAL and NPE), there are differences in propagation path effects that must be taken into account in the comparative studies. In many cases these propagation path differences are negligible. Smoothing over several different observation: will be used to reduce these effects.

III. CHEMICAL/NUCLEAR SOURCE SIMILARITIES AND DIFFERENCES (*NPE* TO *HT* COMPARISON).

The primary purpose of the NPE was to address questions concerning similarities and differences between chemical and nuclear explosions as observed in the seismic wavefield. The experiment was designed to identify seismic source differences between chemical and nuclear sources that could be used to discriminate between the two source types. Such a tool would be invaluable in monitoring a Comprehensive Test Ban Treaty (CTBT).

Figure 1 illustrates the close proximity of the NPE (chemical, 390 m depth) and HT (nuclear, 385 m depth) sources on Rainier Mesa. Each source was observed by the same near-source receiver array thus eliminating local receiver effects in such a comparison. The relative difference of the two source locations (273 m) results in small differences in total propagation distance (30%) for stations 1P, 1A, 2P, 4A, 4P, 7A, 7P, 9A, and 12 while other stations have more significant differences in propagation distance. Figure 3 displays typical Z (vertical), R (radial) and T (transverse) acceleration time series and velocity spectral comparison at station 1A. This figure illustrates the earlier conclusion that phase information is easily contaminated by near-receiver or near-source structure. Significant differences in the time series are observed. In contrast the spectral comparisons show almost identical shapes and amplitudes over the bandwidth of the signal (0.36 to 100 Hz). The presence of a strong transverse component of motion is not consistent with an isotropic model of the source unless the geological structure is represented by a complex three dimensional structure where scattering into the transverse motions is important.

Stochastic comparisons designed to quantify source spectral similarities and differences were completed. The first step in this process was the identification of the bandwidth with acceptable signal to noise ratio. Comparison of the signal spectra to pre-event noise estimates and careful examination of the spectral shape led to a conservatively determined bandwidth of 0.36 to 100 Hz. The second step was the determination of an appropriate frequency domain smoothing window in order to reduce variances in the individual spectral estimates. Various numerical tests of different smoothing windows were performed and a window criteria which minimized the variance and bias of the spectral estimate was selected. A single window was chosen with a width of 3.48 Hz. At low frequencies the window which is centered on the frequency of the spectral estimate is allowed to grow to a width of 3.48 Hz as frequency increases. Figure 4 displays the smoothed spectra for station 1A and the resulting Z, R and T spectral
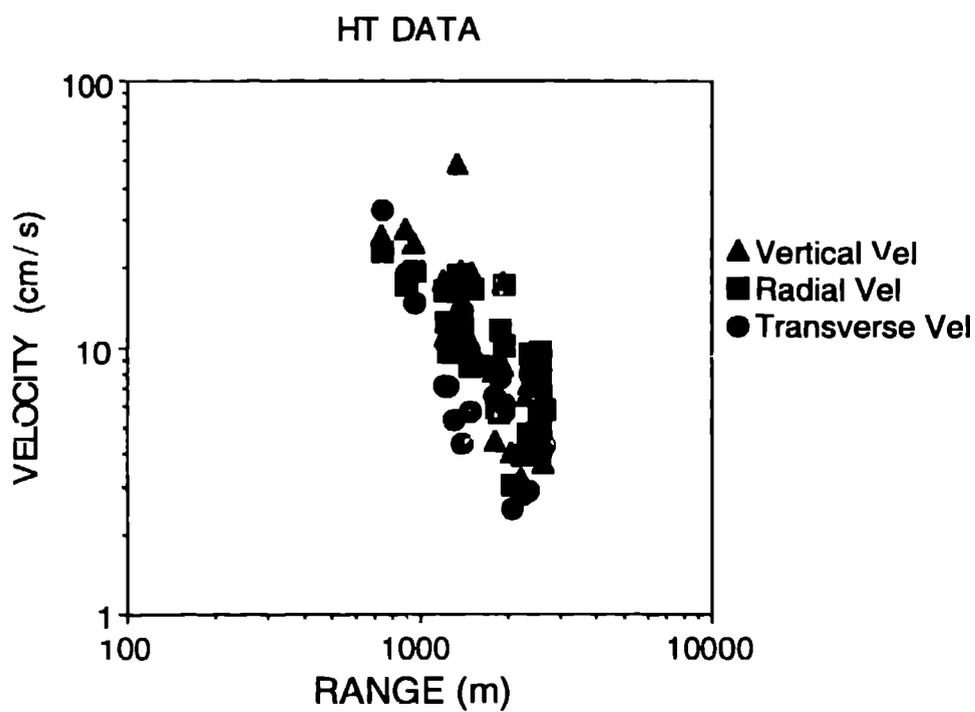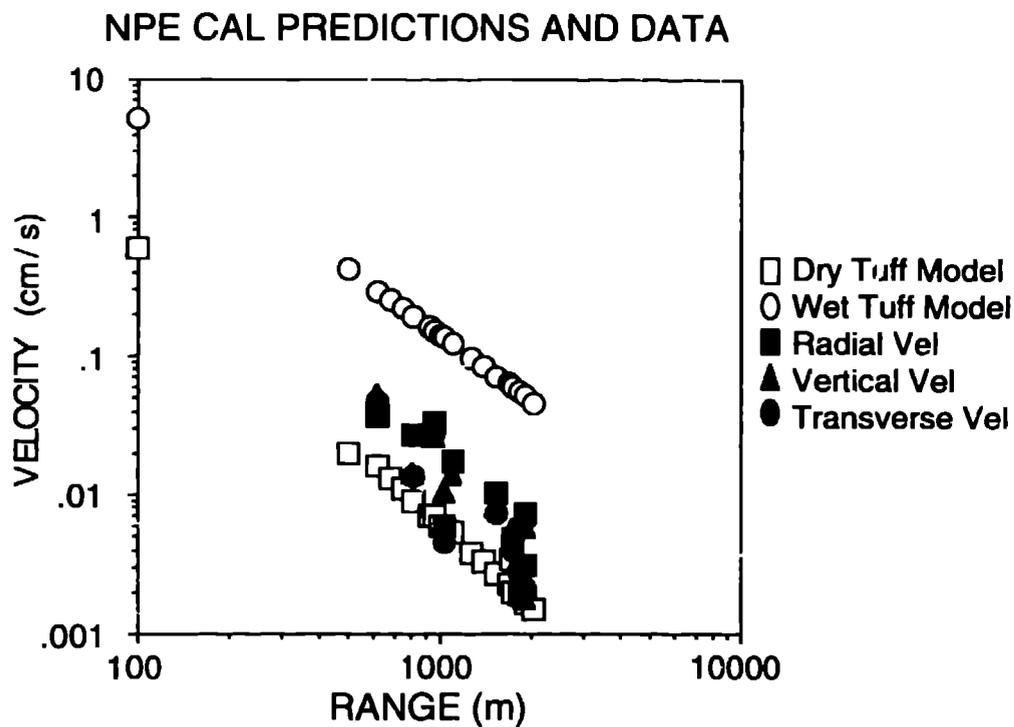
NPE CAL PREDICTIONS AND DATA

HT DATA

Figure 2: Peak velocity data for the radial (R), vertical (Z) and transverse (T) components of surface velocity observed at the stations diagrammed in Figure 1 from the explosions NPE CAL (top) and HT (bottom). Predictions plotted for the NPE CAL (open symbols) are from the models of Perret and Bass (1974).
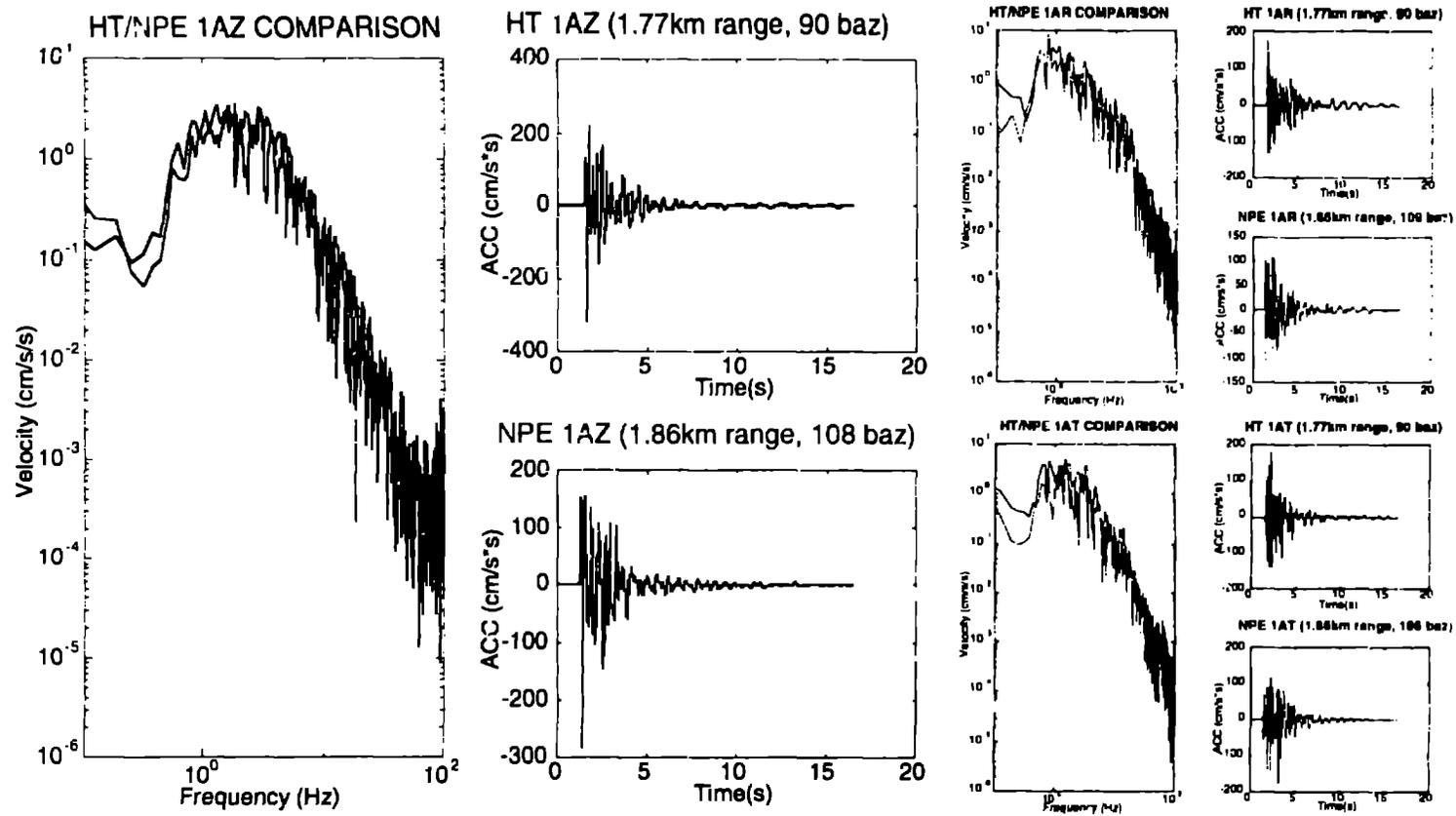
Figure 3: Comparison of the vertical accelerations from HT and NPE at Station 1A (Figure 1) in the time and frequency domain (left). Radial (R) and transverse (T) comparisons made in the smaller format to the right.
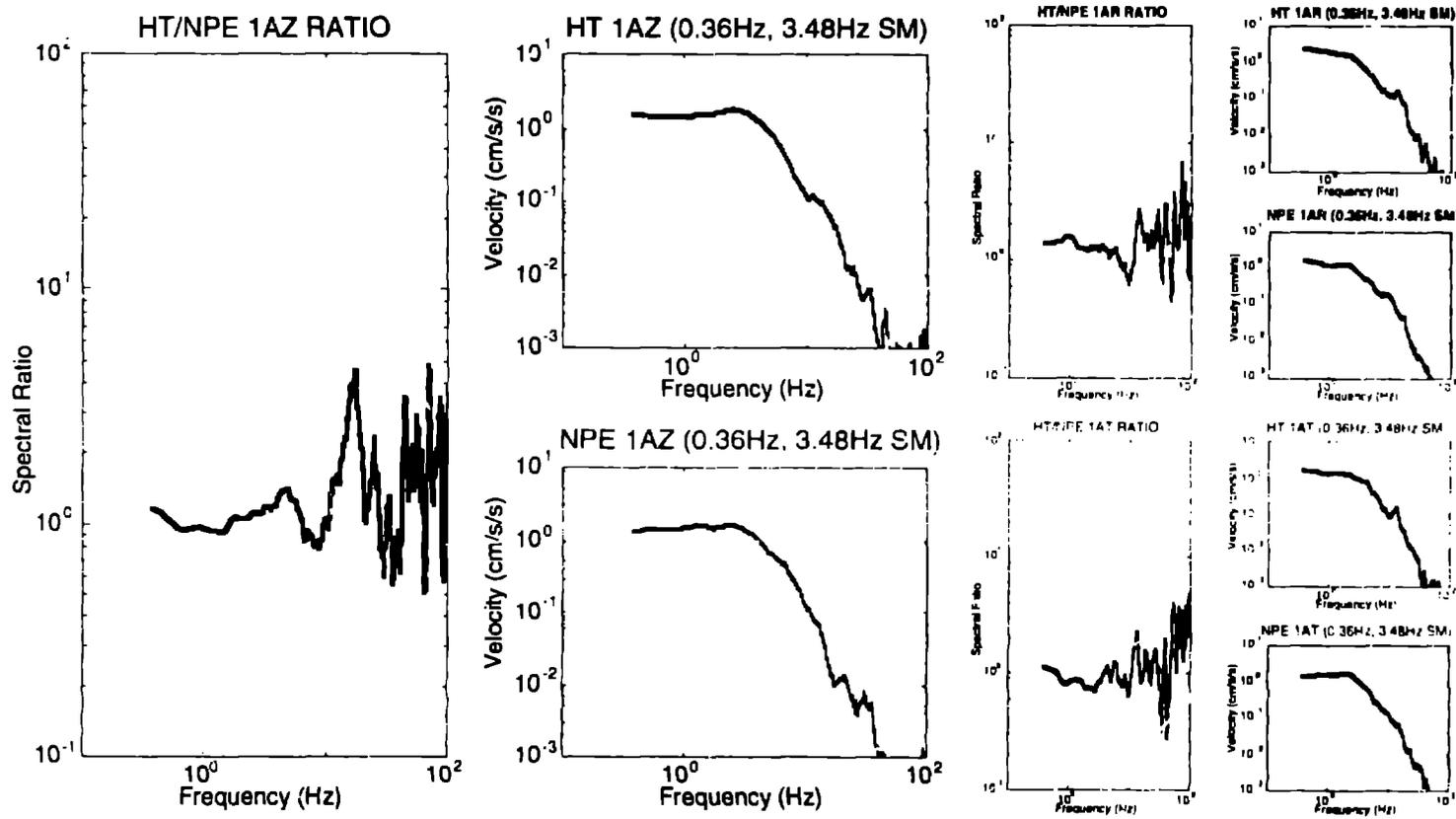
Figure 4: Smoothed spectra (Z to the left and R/T to the right) from HT and NPE at Station 1A (Figure 1) using a 3.48 Hz smoothing window. The spectral ratios (HT/NPE) of the smoothed spectra are also given.

ratios (HT/NPE). These three ratios have gross characteristics that are similar. (1) Flat from 0.36 to 8 to 10 Hz; (2) Low frequency ratio near 1; (3) High frequency ratio that increases with frequency; and (4) Significant high frequency variability.

In order to illustrate the parts of the spectral ratio characteristics that were source-station independent, the ZRT ratios from each station were combined into a single station dependent estimate, Figure 5. The mean (solid line) and log normal variance illustrates the small scatter in the low frequency estimates and the increased scatter with increasing frequency. The increase in variance occurs at 5 to 10 Hz. Taking a phase velocity of 2 km/s, the wavelength at which the scatter increases is 200 to 400 m, approximately the scale of the source separation. Arguing that the high frequency structure in the spectral ratio is a result of source location differences, the shape of the ratios for stations 'A and 2P (closest to one another) are similar, rising at high frequency, while the more distant station, 7P, decreases at high frequency (Figure 1).

If the high frequency variation in spectral ratios is a reflection of the different locations of HT and NPE, as seen at each receiver then one might expect to average these differences by smoothing over a number of observations at different azimuths. Figure 6 displays the smoothed all component spectral ratio using all station pairs with propagation path differences of no more than 30%. The high frequency variations observed in the single components and single stations are eliminated although the variances in the spectral ratios increase with frequency as expected from the stochastic model.

This analysis defines significant source location related propagation path differences for the HT to NPE comparison in the near-source data. These variations can be smoothed to emphasize source processes. The resulting spectral comparison between NPE and HT is flat from 0.36 to 100 Hz with the ratio of the source strengths equal to 1. *There appear to be no significant spectral differences between this chemical and nuclear source in the near-source region from 0.36 to 100 Hz after stochastic propagation path effects are taken into account.*

IV. UTILITY OF SMALL SCALE CALIBRATION EXPLOSIONS FOR SOURCE QUANTIFICATION (*NPE CAL* TO *NPE* COMPARISON).

In order to quantify propagation path effects expected from the NPE and exercise the data acquisition systems, a small, 300 lb. (C-4), charge was emplaced and detonated at the center of the planned NPE source cavity prior to its excavation. This small source provided the opportunity to test the empirical Green's function approach to source scaling in the near-source region. Since the source was nearly four orders of magnitude smaller than the NPE and the dynamic range of the accelerometers (used for recording the NPE, HT, MQ) were limited, a set of Sprengnether S-6000, 2 Hz seismometers were used to record the NPE CAL at the same locations where the accelerometers were fielded for the other explosions. The instrument corner of the seismometer is in the band of interest for source comparisons, therefore this well known instrument response was taken into account prior to any spectral comparisons.

The smaller NPE CAL waveforms have a higher corner frequency, longer temporal duration, and more complexity than those observed from the NPE. Spectral comparisons in velocity illustrate the four orders of magnitude difference in spectral level at low frequencies, the order of magnitude difference in source corner frequency and the 0.48 to 100 Hz bandwidth of the data. Since the centroids of the NPE and NPE CAL sources are identical there should be no differences in propagation path effects for the two sources as long as the point source representation is appropriate. If secondary source processes such as spall are important contributors to the NPE waveforms, this assumption may not be valid. In order to improve the statistical significance of the source comparisons, the observed spectral ratios for all the Z, R, T and combined single station estimates were averaged as done in the previous analysis. The averaged ratio for NPE/NPE CAL is displayed in Figure 7. Unlike the HT/NPE comparison there are only small increases in variance of the ratios with frequency. This increase in variance with frequency in the previous case was explained in terms of the difference in propagation path between the two sources to be compared. In the NPE/NPE CAL comparison there is little difference in the propagation paths thus resulting in the reduced high frequency variances. Differences in the spatial extent of the two sources and secondary source contributions may be responsible for the slight increase in variance with frequency observed in this case.

As found for the HT/NPE comparisons, all the averaged results (Z, R, T and combined) produce a common source comparison. This result indicates that the generation of the transverse energy scales linearly with source size. One might conclude that this observation is consistent with a linear scattering mechanism for the generation of transverse energy.
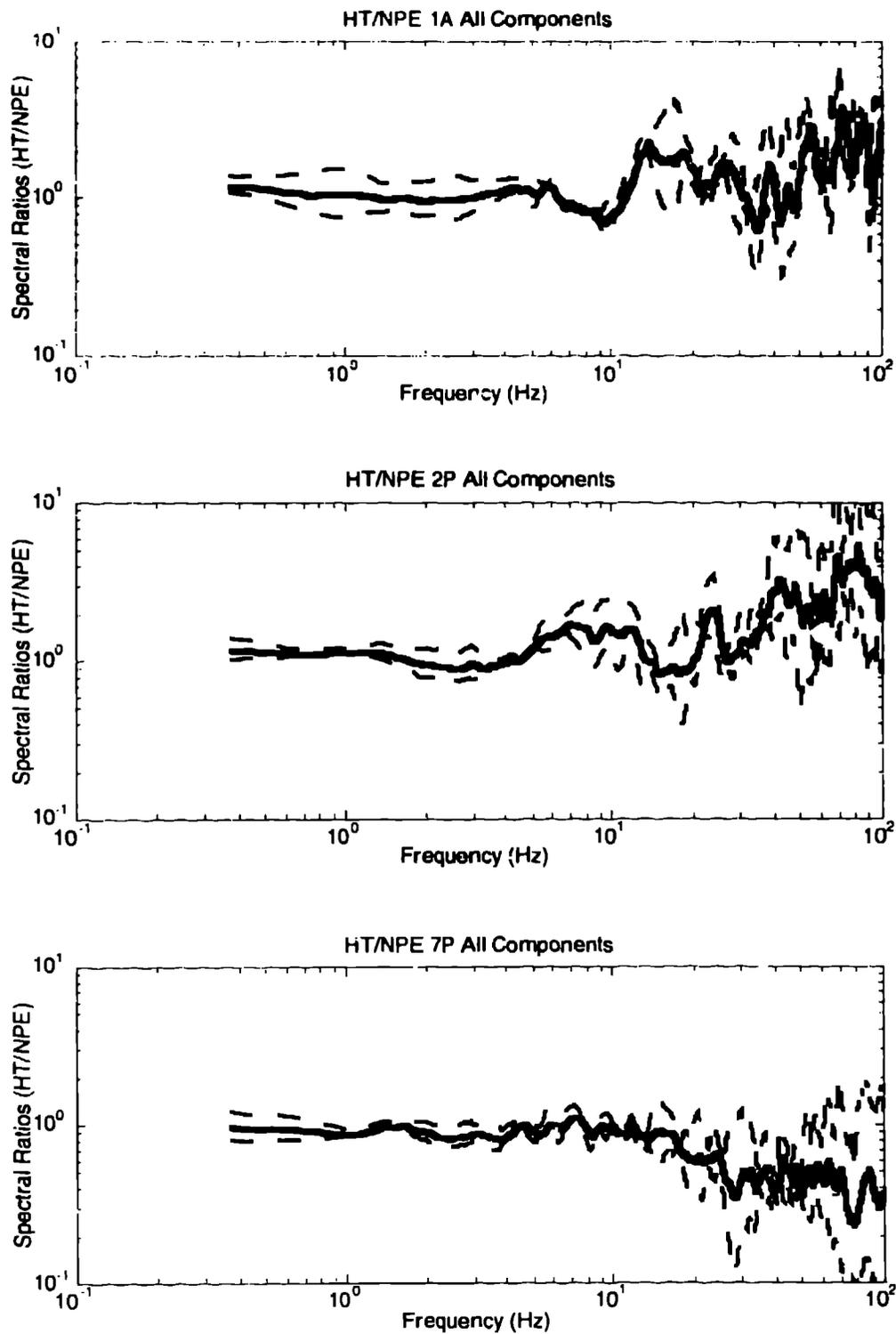
Figure 5: Mean spectral ratios (radial, vertical and transverse) at Stations 1A, 2P and 7P (Figure 1) for the explosions HT and NPE plotted as a solid line. The plus and minus one standard deviation (log normal) of the mean spectral ratio estimate is also plotted as a dashed line.
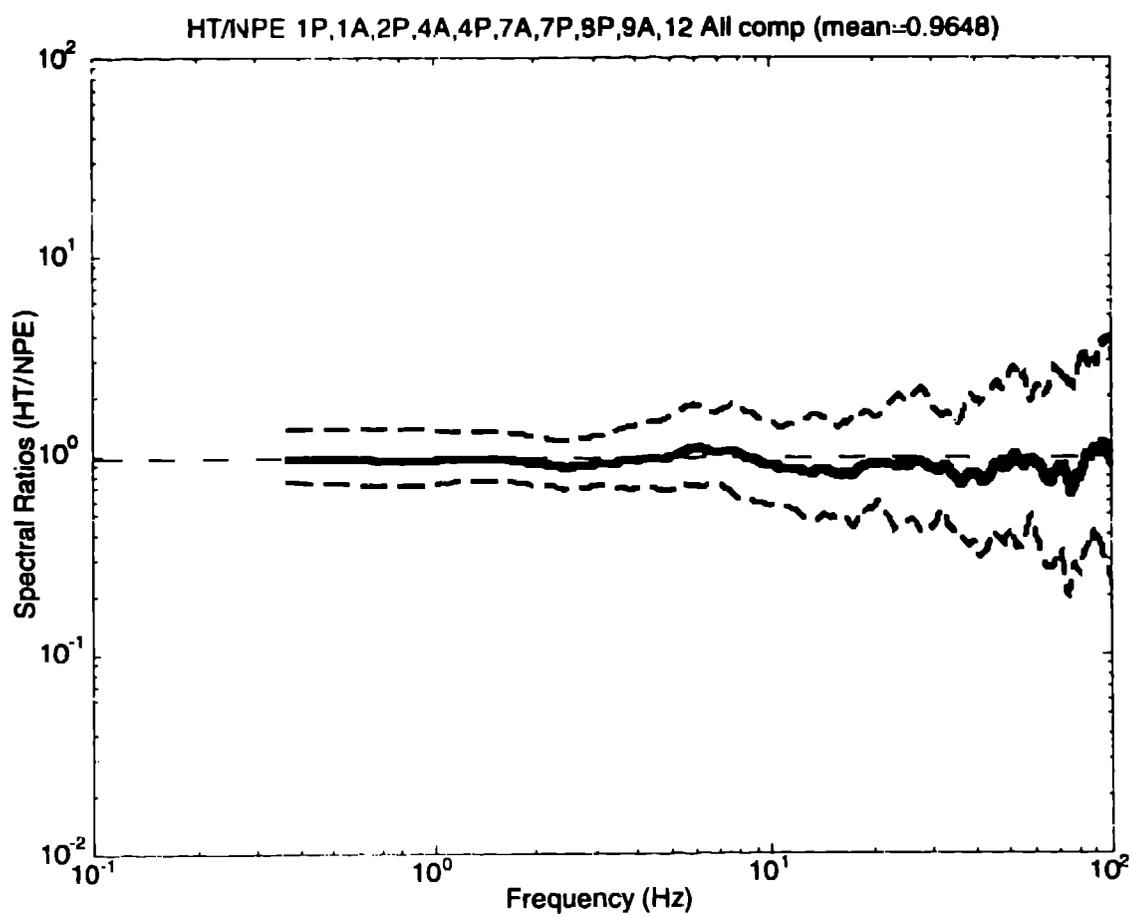
Figure 6: Mean spectral ratio (HT/NPE) determined averaging all station pairs (propagation path differences < 30%) and all components. Again the solid line is the mean with the p! 's or minus one standard deviation (log normal) characterizing the scatter in the individual estimates plotted as a dashed line.

These NPE/NPE CAL comparisons (Figure 7) support a 10^4 source difference between the two sources at long periods, a source corner for NPE near 2 Hz, f^{-2} spectral decay between corners and a corner frequency of 50-60 Hz for the NPE CAL. Comparison of these smoothed results with those from theory will be given in Section VI.

V. EXPLOSION SOURCE SCALING OF SMALL YIELD NUCLEAR EXPLOSIONS (HT TO MQ COMPARISON).

The last set of empirical comparisons allows the investigation of source differences between the two nuclear explosions MQ and HT. As Figure 1 indicates, the two sources are to the north of the testing area. Propagation path distance differences from the two sources to the stations to the south are small. This data provides the opportunity for quantifying differences in propagation path as well as differences in absolute source location. As was done in the case of the HT/NPE comparisons, all source-receiver distances that were no more than 30% different for the two sources were used to produce a combined smoothed spectrum (Figure 8). This ratio begins at low frequency with a value near 0.4 and rise to a plateau of 1 at 5 to 6 Hz. The variances in the ratio estimates increase as a function of frequency above 5 Hz just as observed in the HT/NPE comparisons.

A number of stations in the free surface array (6P, 6A, 7P, 7A, 8P, 9A, 10P) have propagation path differences between the two sources of less than 10%. These more limited data were used to estimate a second spectral ratio along with variances (Figure 9). The spectral variance estimates in this second set are dramatically reduced from those of the more inclusive data set. The resulting spectral ratio mean is nearly identical to the previous estimate. This result argues that much of the low frequency variation in the spectra (<5 to 10 Hz) is attributable to propagation path differences observed in the near-source region from these explosion sources. The higher frequency variations may be a result of near-source differences like the near receiver variations observed in the array measurements from a single source and reported by Reinke *et al.*, these proceedings.

The HT/MQ spectral ratios is consistent with an interpretation that the MQ explosion was larger than the HT explosion. This source size difference is reflected in the long period spectral ratio HT/MQ of 0.4. The source spectra for the two explosions merge at frequencies greater than 5 Hz above the corner frequency for each explosion.

VI. SOURCE MODELS

The comparison of *NPE to NPE CAL* documents the strong yield effect between the 300 lb. C-4 calibration explosion (390 lb. equivalent TNT) and the 1 kiloton (kt) (equivalent TNT) NPE. In order to interpret these yield effects a set of Mueller Murphy source functions for wet tuff were calculated using the following material properties for the source region:

P Velocity	2.20 km/s
S Velocity	1.27 km/s
Density	1.85 gm/cc
Depth	400 m

RDP's for sources of 2, 1, and 0.00022 kt were calculated. These source functions which are calculated in the frequency domain provide the opportunity for comparison to the experimental source differences determined in the analysis of the data. Figure 10 compares spectral ratios of the 2/0.00022 kt and of the 1/0.00022 kt with the observed NPE/NPE CAL spectral ratios. The comparisons between the models and the data validate the Mueller-Murphy source model for wet tuff and suggest that source models with yields between 1 and 3 kt best describes the NPE/NPE CAL data. The long period spectral level difference, NPE corner frequency and NPE CAL corner frequency are all well replicated by the Mueller-Murphy source model.

The empirical data is consistent with the scaling relations incorporated into the Mueller-Murphy source model. It appears that this model is appropriate for wet tuff over the four orders of magnitude of yield represented by the NPE CAL and NPE explosions. The Mueller-Murphy model was developed for nuclear sources. The mean of the range of acceptable source models suggests that there is an approximate factor of two difference between nuclear and chemical coupling at large yields. This conclusion does not call upon a factor of two coupling enhancement for the smaller NPE CAL explosion.

Two alternate explanations for the apparent factor of two enhanced coupling for the NPE can be introduced. It is difficult to separate overshoot from long period spectral level with limited bandwidth data. If the NPE had
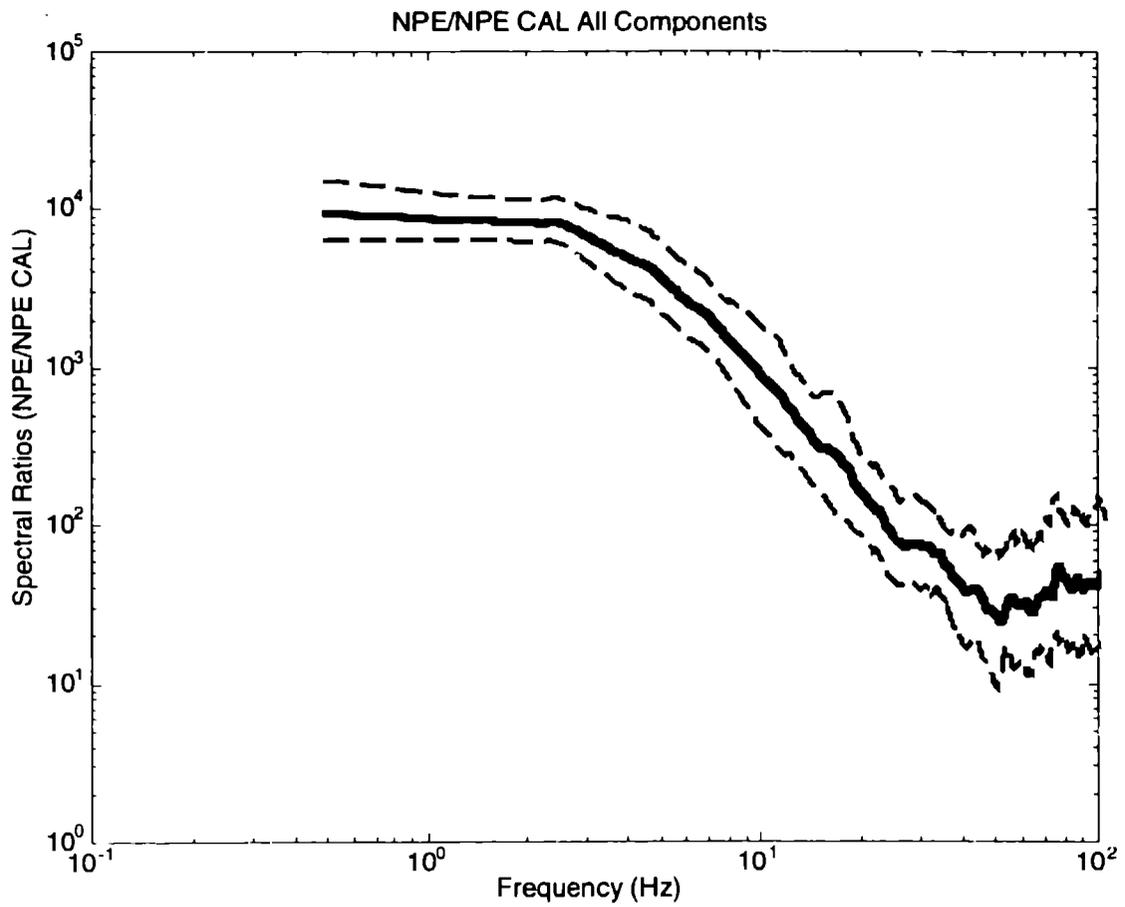
Figure 7: Mean spectral ratio (NPE/NPE CAL) determined averaging all station pairs (propagation path differences < 30%) and all components. Again the solid line is the mean with the plus or minus one standard deviation (log normal) characterizing the scatter in the individual estimates plotted as a dashed line.
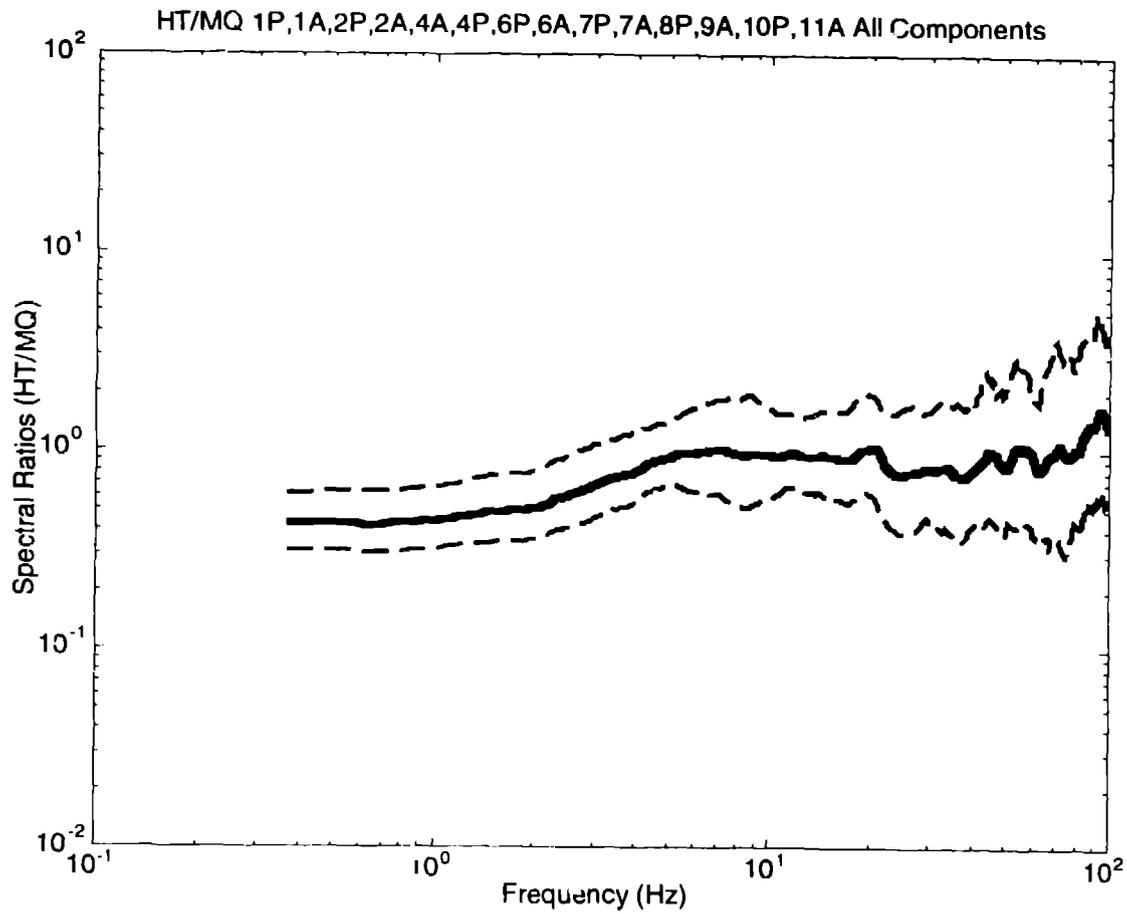
Figure 8: Mean spectral ratio (HT/MQ) determined averaging all station pairs (propagation path differences < 30%) and all components. Again the solid line is the mean with the plus or minus one standard deviation (log normal) characterizing the scatter in the individual estimates plotted as a dashed line.
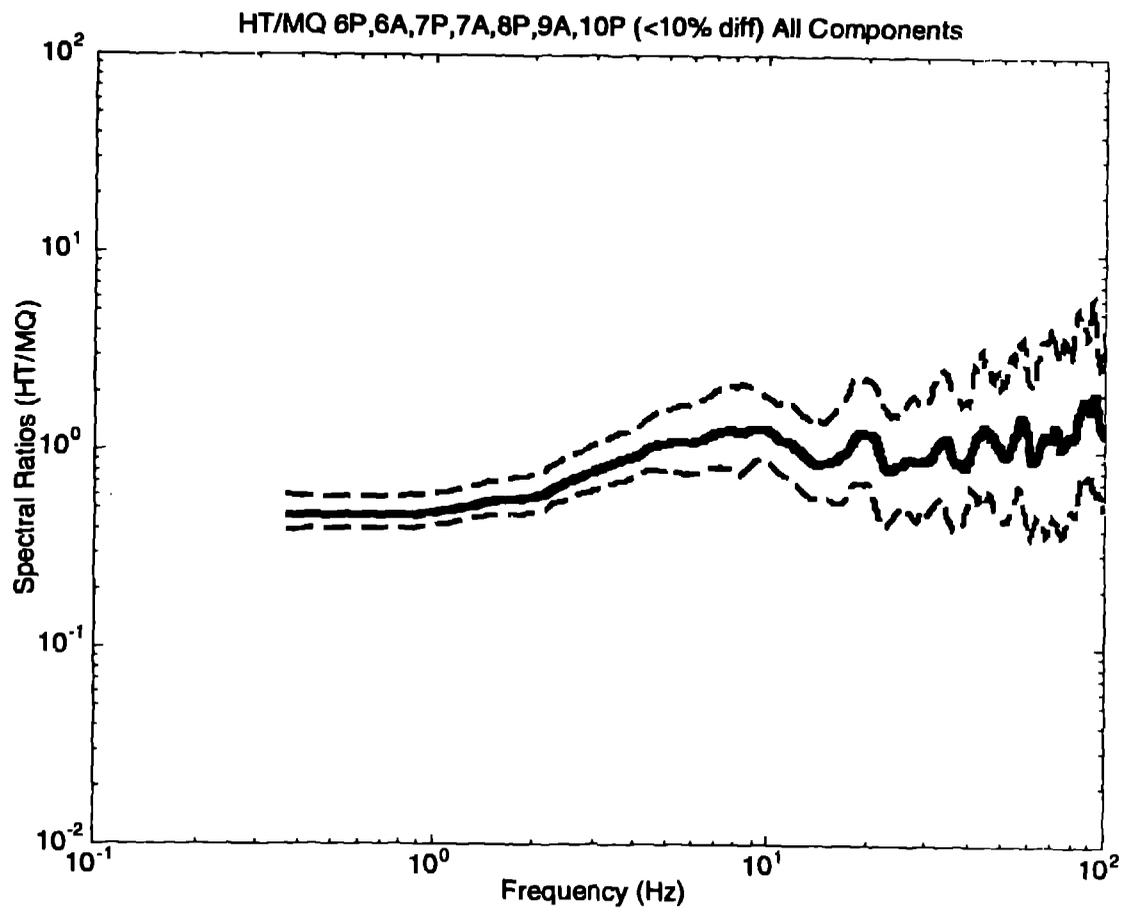
Figure 9: Mean spectral ratio (HT/MQ) determined averaging all station pairs (propagation path differences < 10%) and all components. Again the solid line is the mean with the plus or minus one standard deviation (log normal) characterizing the scatter in the individual estimates plotted as a dashed line.
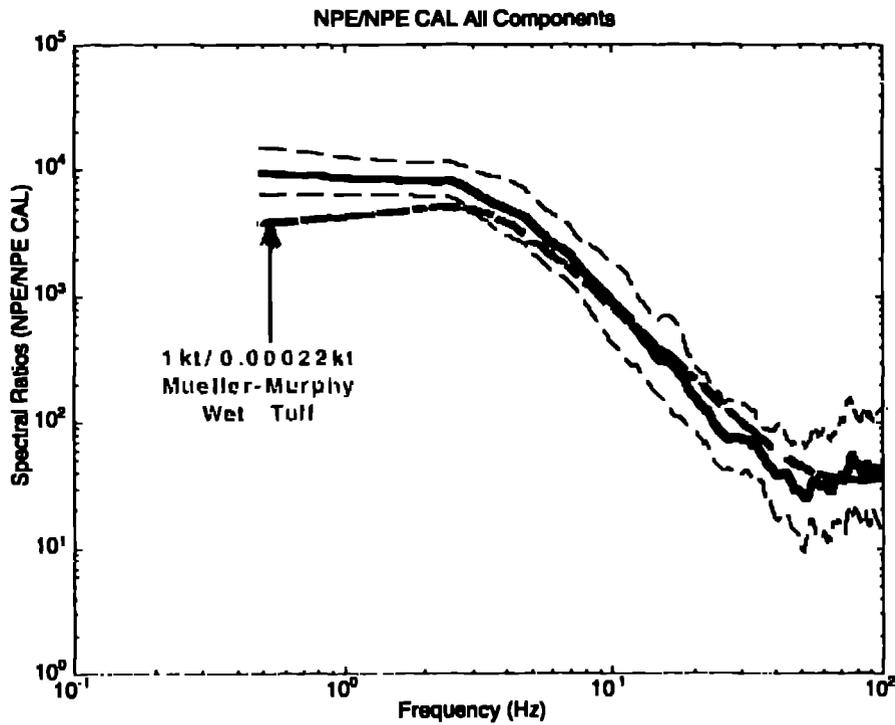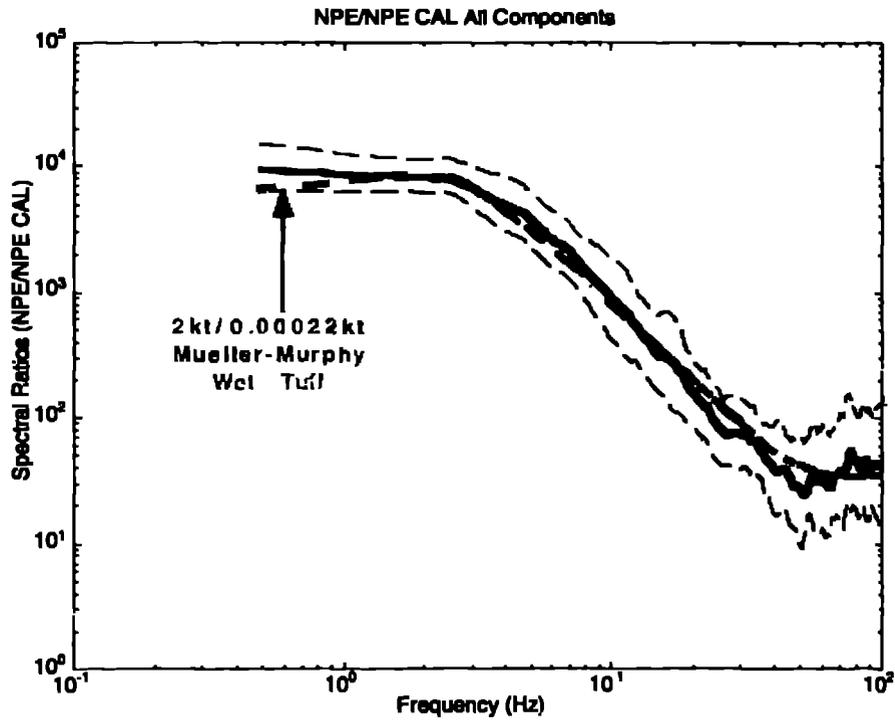
Figure 10: Comparison of the predict d spectral ratics from the Mueller-Murphy wet tuff model (thick/light dashed lines) and the NPE/NPECAL empirical data (thick dark line) for model yields of 1 and 2 kt.

significant overshoot associated with the source time function, then the limited bandwidth analyzed in this study would be unable to separate overshoot from the enhanced coupling postulated for the chemical explosion.

The NPE CAL explosion, since it was detonated at the same depth as the NPE, was highly overburied. This small explosion resulted in no surface spallation. The NPE although also overburied did spall at surface ground zero and so the possibility exists for secondary source contributions from spall to the NPE seismic source function. If these contributions boost spectral levels below the source corner frequency then this effect could also be interpreted as enhanced coupling for the chemical explosion. The fact that the NPE itself was overburied and that observed dwell times at surface ground zero were much less than 1 sec in duration argues that this secondary source effect was probably minimal.

VII. CONCLUSIONS

In the near-source region there are no apparent spectral differences between *HUNTERS TROPHY and THE NON-PROLIFERATION EXPERIMENT* in the bandwidth of 0.36 to 100 Hz. Figure 6 demonstrates the flat spectral ratio for these two events with a mean value of 0.96. Although the variance of the spectral ratio estimate increases as frequency increases the mean value shows little departure from the value of 1 across the entire bandwidth of the data. These results indicate that there is little information in the near-source wavefield that can be used to distinguish chemical from nuclear explosions. Although this result suggests that seismic waves cannot be used to discriminate nuclear explosions from chemical explosions, it also supports the use of large chemical explosions to replicate nuclear explosion effects. One could imagine a series of chemical explosion experiments to quantify source phenomenology, near-source material property effects, and regional explosion effects in areas where only earthquakes have been observed in the past.

Comparison of the empirical spectral ratios for the NPE and the NPE CAL suggest that the NPE is best replicated by a Mueller-Murphy model with a yield of about 2 kt. This conclusion is made in light of alternate interpretations in terms of source overshoot or spall contributions. The empirical data supports a Mueller-Murphy source time function for wet tuff. These comparisons also suggest that this model for wet tuff is extendible to quite small yield explosions. The yield of the NPE CAL is comparable in size to individual detonations in ripple fired mining explosions. This result suggests that a good starting point for such source models might be the Mueller-Murphy source time function, recognizing that the geometry for the NPE CAL is not the same as the cylindrical geometry of typical mining explosions. The source time function predicted by the Mueller-Murphy model may be appropriate but the geometrical effects of the mining explosions may be quite different. One would expect enhanced shear wave generation by the mining explosions.

The raw data display strong first order propagation path effects which must be taken into account prior to making any source comparisons. It was only because all these different types and sizes of sources were recorded by the same receiver array that this source comparison study could be undertaken. Even with the suite of constant receiver sites for the different sources significant spectral smoothing was necessary across neighboring frequency points and across different receiver sites in order to appropriately reduce the variances in the spectral estimates resulting from slightly different propagation paths from the different sources and variances introduced by the spectral estimation procedure.

In the case of Figure 6, thirty individual waveforms from each of the two explosions went into the spectral ratio estimate. It is not often in comparative source studies that redundancy in near-source observations of this magnitude are available. The spectral ratios calculated for the HT/MQ comparisons indicate that the number of observations in the averaging process can be reduced if the propagation path differences between the two sources are reduced. Comparison of Figures 8 and 9 indicates that if propagation path differences can be reduced to less than 10% (assuming the same receiver site) that statistical stable spectral ratios can be made to frequencies below 1 Hz with significantly fewer components. Variances at frequencies above 10 Hz are still large in this case as the wavelengths of this energy become equal to or shorter than the difference in propagation path.

In all comparisons (HT/NPE, NPE/NPE CAL, and HT/MQ) the analysis of transverse components of motion produced results that were identical to those from the radial and vertical components of motion. The mechanism for SH generation must be linked to the source function in the same way that the P and Sv waves(radial and vertical motions) are linked. A linear scattering mechanism for the generation of transverse motions is consistent with these observations. These results suggest that the transverse component of motion receives a strong source imprint very close to the explosion.

ACKNOWLEDGMENTS

REFERENCES

Mueller, R. A. and Murphy, J. R., 1971. Seismic characteristics of underground nuclear detonations. Part I. Seismic scaling law of underground detonations, *Bull. seism. Soc. Am.*, *61*, 1675-1692.

Perret, W. R. and Bass, R. C., 1974. Free-field ground motion induced by underground explosions, SAND74-0252, Sandia National Laboratories, Albuquerque, New Mexico.